



Hydrated $\{\text{Mo}_{72}\text{Fe}_{30}\}$ clusters: Low-frequency hydrogen modes and self-aggregation

Emiliano Fratini^a, Antonio Faraone^{b,c}, Ana Maria Todea^d, Piero Baglioni^{a,*}

^a CSGI and Department of Chemistry, University of Florence, 50019 Florence, Italy

^b National Institute of Standards and Technology (NIST) Center for Neutron Research, Gaithersburg, MD 20899, USA

^c Department of Materials Science and Engineering, University of Maryland, College Park, MD 20742, USA

^d Fakultät für Chemie, Universität Bielefeld, 33615 Bielefeld, Germany

ARTICLE INFO

Article history:

Available online 17 July 2010

Dedicated to Achim Muller

Keywords:

Polyoxomolibdate

Water dynamics

QENS

INS

SAXS

Nanocapsules

ABSTRACT

Using incoherent quasi-elastic and inelastic neutron scattering, we have investigated the hydrogen relaxational dynamics and hydrogen vibrational modes in the polyoxomolybdate specie $[\text{Mo}_{72}\text{Fe}_{30}\text{O}_{252}(\text{CH}_3\text{COO})_{12}[\text{Mo}_2\text{O}_7(\text{H}_2\text{O})]_2[\text{H}_2\text{Mo}_2\text{O}_8(\text{H}_2\text{O})](\text{H}_2\text{O})_{91}] \cdot \approx 150 \text{ H}_2\text{O}$. The translational dynamics of the water molecules in the compound is profoundly different from that of bulk water at the same temperature showing a non-Debye relaxation behavior. The temperature dependence of the relaxation time can be described in terms of an Arrhenius law, indicating that the dynamics is triggered by the breaking of the bonds connecting the crystal water molecules with the hydrophilic nanocapsule surfaces. Inelastic neutron scattering spectra confirm the attenuation of water translational modes with respect to the bulk water case due to the strong destructuring effect imposed by the nanocage interface and the enhancement of the highest frequency librational mode as already found in hydrated Vycor or Gelsil matrix. Small angle X-ray scattering on freshly prepared aqueous solution evidences the presence of nanocapsule structures proper of the monomer (2.6 nm in diameter) that coexist with a small amount of oligomers. After 1 month the polyoxomolibdate specie self-assembles in a supramolecular structure with a polydisperse distribution of dimensions spanning from the monomer to the “blackberry” vesicular structure already reported in literature.

© 2010 Elsevier B.V. All rights reserved.

1. Introduction

Polyoxometalate (POM) clusters represent a class of inorganic compounds showing unique properties and a wide range of applications having relevance to catalysis, materials science and medicine [1]. Their molecular properties such as composition, size, shape, charge density, acidity, and solubility can be extensively tailored in order to match different requirements. As an example, the icosahedral cluster $[\text{Mo}_{72}\text{Fe}_{30}\text{O}_{252}(\text{CH}_3\text{COO})_{12}[\text{Mo}_2\text{O}_7(\text{H}_2\text{O})]_2[\text{H}_2\text{Mo}_2\text{O}_8(\text{H}_2\text{O})](\text{H}_2\text{O})_{91}] \cdot \approx 150\text{H}_2\text{O}$ is attractive because it has a peculiar hydrophilic surface and is a novel polyprotic nanoacid [2,3]. The cluster thereafter shortly referred as $\{\text{Mo}_{72}\text{Fe}_{30}\} \cdot \approx 150\text{H}_2\text{O}$ or simply $\{\text{Mo}_{72}\text{Fe}_{30}\}$, exhibits a nanometer-sized cavity and 20 pores equivalent to 20 $\text{Mo}_3\text{Fe}_3\text{O}_6$ rings. It can be considered as a nanocapsule with a diameter of about 2.5 nm. The icosahedral cluster contains 91 water ligands coordinated to the Fe and Mo atoms (40 outside and 51 inside). In addition, about 150 discrete H_2O molecules are present, 25 inside the nanocavity and the rest in the voids between the clusters. On the other hand, the $\{\text{Mo}_{72}\text{Fe}_{30}\}$ cluster has unique solution properties: its acid nature, $\text{Fe}^{\text{III}}(\text{H}_2\text{O})$ groups are weakly acidic, results in the formation of

discrete spherical macroanions. These macroanions self-assemble into “blackberry”-type structures where as an example their dimension can be controlled by the pH value [2–6]. In this paper, we report on the single particle dynamics of both, water molecules located inside and attached to the $\{\text{Mo}_{72}\text{Fe}_{30}\}$ nanocapsule by incoherent Quasi-Elastic Neutron Scattering (QENS). Moreover, we show data on water low-frequency modes as accessed by Inelastic Neutron Scattering (INS). In the last section of the paper, we address solution structure and self-assembly properties of such macroanions using Small Angle X-ray Scattering (SAXS).

2. Experimental

2.1. Materials

The investigated sample was prepared according to a published preparation method [7].

2.2. QENS measurements

QENS measurements of $\{\text{Mo}_{72}\text{Fe}_{30}\}$ nanocapsules have been performed at the National Institute of Standards and Technology (NIST) Center for Neutron Research (NCNR), using the disk chopper

* Corresponding author.

E-mail addresses: baglioni@csgi.unifi.it, piero.baglioni@unifi.it (P. Baglioni).

spectrometer (DCS) [8] and the high-flux backscattering spectrometer (HFBS) [9]. A detailed description of the instrumental set-up can be found elsewhere [10]. DCS was operated in the “low resolution” configuration using neutrons with 9 Å incoming wavelength. Thus, the instrumental resolution function was a Gaussian Function with ≈ 20 μeV Full Width at Half Maximum (FWHM), as measured using both a vanadium standard and a measurement of the sample itself at ≈ 20 K, a temperature at which the hydrogen atoms dynamics in the sample is frozen. Data were collected from 300 K to 250 K, with 10 K intervals. The backscattering spectrometer was operated with a Doppler frequency of 50 Hz which gives an energy resolution of ≈ 1 μeV and an accessible energy window of ± 36 μeV . Data were collected at 250 K, 240 K, and 230 K.

2.3. INS measurements

INS data were obtained using the Filter Analyzer Neutron Spectrometer (FANS) on BT-4 [11] at the NCNR. The sample was arranged in an annular geometry and contained in an aluminum can. The temperature was controlled using a closed cycle refrigerator with an accuracy better than 0.1 K. Two different monochromators were used in order to access energy transfers between 4 meV and 140 meV: pyrolytic graphite PG(0 0 2) that covers from 4 meV to 45 meV and Cu(2 2 0) in the range from 25 meV to 250 meV. Samples prepared identically to those used in the QENS experiment were analyzed. Data were collected over the energy range from 5 meV to 140 meV at 200 K and 270 K.

The INS spectra collected on FANS for each sample are representative, within certain approximations, of the density of states of the sample [12]. DAVE¹ was used for the data reduction of the INS data. The spectrum for the hydrogen density of state in {Mo₇₂Fe₃₀} nanocapsules was modeled using 8 Gaussian lineshapes as detailed in the text (see Fig. 3).

2.4. SAXS measurements

SAXS measurements were carried out with a HECUS SWAX-camera (Kratky),² detailed explanation of the experimental set-up can be found elsewhere [13]. The Kratky camera was calibrated in the small angle region using silver behenate ($d = 58.38$ Å) [14]. Scattering curves were obtained in the Q -range between 0.009 Å⁻¹ and 0.55 Å⁻¹, Q being the scattering vector $Q = (4\pi \sin\theta)/\lambda$, 2θ the scattering angle, and λ is the wavelength of the incoming photons (or neutrons). Aqueous solution of (0.5 mg/mL) {Mo₇₂Fe₃₀} nanocapsules was filled into a 1 mm quartz capillary and kept at 25 °C. This concentration has been chosen in order to stay above the reported critical association concentration (CAC) [5], reduce the counting time and to avoid any unwanted inter-monomer interference. SAXS experiment was performed both on the freshly prepared and on the 1 month old solution. During the measurement the temperature (25 °C) was controlled by a Peltier element, with an accuracy of ± 0.1 °C. In order to reduce the noise on the scattering curves the total counting time has been fixed to 9 h as repetition of three consecutive acquisitions of 3 h. The averaging was acceptable since consecutive acquisitions on the same sample presented the same scattering trend. For this reason SAXS curve for the fresh sample are representative of a 3 h old sample. All scattering curves were corrected for the empty cell/solvent contribution considering the relative transmission factor. SAXS curves were iteratively desmeared using the procedure reported by Lake [15].

¹ DAVE, National Institute of Standards and Technology Center for Neutron Research.

² Identification of a commercial product does not imply recommendation or endorsement by the National Institute of Standards and Technology, nor does it imply that the product is necessarily the best for the stated purpose.

3. Results and discussion

3.1. Hydrogen relaxational dynamics and vibrational modes

The QENS spectra were fitted, in the range from $Q \approx 0.2$ Å⁻¹ to $Q \approx 1.3$ Å⁻¹ where the spectra are mostly determined by the center of mass dynamics of the water molecules, using the sum of a delta function and of the Fourier transform of a stretched exponential function, plus an instrumental background. The fitting formula was:

$$S(Q, \omega) = \text{Amp} \left\{ x\delta(\omega) + (1-x)FT \left\{ \exp \left[-\left(\frac{t}{\tau} \right)^\beta \right] \right\} \right\} + bkg \quad (1)$$

The delta function was identified as the contribution of the 91 water molecules which are part of the nanocage. In fact, x is Q independent indicating that the delta is not related to a rotational or confined process. At the same time, the value of $x \approx 0.40$ is in agreement with the amount of scattering originating from the water molecules within the {Mo₇₂Fe₃₀} nanocluster. Finally, x is temperature independent [10]. The QENS results indicate that this population of water molecules has a dynamics much slower than 1 ns (corresponding to the energy resolution of the spectrometers) at the length scales (of the order of the Å) investigated in the experiment.

The value of the stretching exponent $\beta \approx 0.46$, was found to be with good accuracy both Q and T independent [10]. In Fig. 1 we report the value of the average relaxation time, $\langle \tau \rangle = \tau(Q)\beta^{-1}\Gamma(1/\beta)$, at $Q \approx 1$ Å⁻¹, $\Gamma(u)$ being the Gamma function. The data can be well fitted according to an Arrhenius law, $\langle \tau \rangle = P \times \exp[-E_A/RT]$ with the prefactor $P = 5.9 \times 10^{-7}$ ps $\pm 1.5 \times 10^{-7}$ ps, and an activation of $E_A = 46.8$ kJ/mol ± 0.6 kJ/mol.

The Q dependence of the average relaxation time indicates a diffusive type of relaxation process. Therefore from the whole of the data obtained in the QENS region, we can conclude that the ligand water molecules in the nanocage are strongly bounded to the cluster and do not show any translational dynamics. On the other hand, the crystal water hydrating the nanocage show a diffusive process which is thermally activated by the breaking of one or more hydrogen bonds. The spectra indicate a broad distribution of relaxation

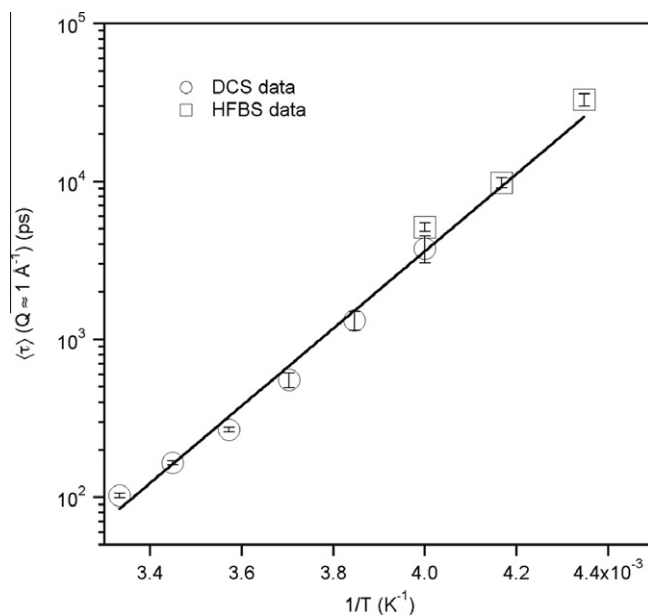


Fig. 1. Temperature dependence of the average relaxation time measured at $Q \approx 1$ Å⁻¹. The continuous line is a fit to an Arrhenius law. Error bars represent the standard deviation.

times, likely related to the variety of microscopic environments sampled by the water molecules around the cage.

According to the literature on bulk, supercooled and confined water [16–19] the low-frequency portion of INS spectra for water molecules ($E < 150$ meV) can be considered as the sum of two translational (at about 8 meV and about 20 meV) and three higher-frequency librational bands [20] (from 40 meV to 150 meV). It is common that the librational bands, resulting in a broad feature centered below 150 meV, are enhanced with respect to the translational ones. In the present case of water confined in $\{\text{Mo}_{72}\text{Fe}_{30}\}$ nanocapsules, four components need to be added in order to consider the contribution coming from the methyl group present in the acetate ligand stabilizing the spherical “Keplerate”: these Gaussians are used to fit the region from 10 meV to 40 meV [21]. The presence of the acetate ligands renders the determination of the second translational contribution coming from the water molecules unfeasible so that only the other four components (one for the low-frequency translation and three for rotations/librations) have been used. For this reason the component at 20 meV will not be commented as well as the four methyl bands between 10 meV and 40 meV are outside the scope of this investigation.

In Fig. 2 the evolution of low-frequency INS concerning water in $\{\text{Mo}_{72}\text{Fe}_{30}\}$ samples is shown as a function of temperature and the relative fitting curve using eight Gaussian components is reported. If we exclude the methyl contribution the incoherent neutron spectrum of water bonded to the $\{\text{Mo}_{72}\text{Fe}_{30}\}$ nanocage is dominated by rotational dynamics as already reported in hydrated systems like Vycor [22] or Gelsil [18] where the water is confined in the matrix nanopores. As temperature decreases, the high frequency component of the broad band centered at about 90 meV is enhanced in amplitude.

In order to have a detailed description of the fine structure of the low-frequency vibrational density of states, the INS spectra have been fitted according to the equation:

$$\text{INS}(E) = \sum_{n=1}^8 \frac{A_n}{\sqrt{2\pi}\sigma_n} \exp\left(\frac{E - E_n}{2\sigma_n^2}\right) \quad (2)$$

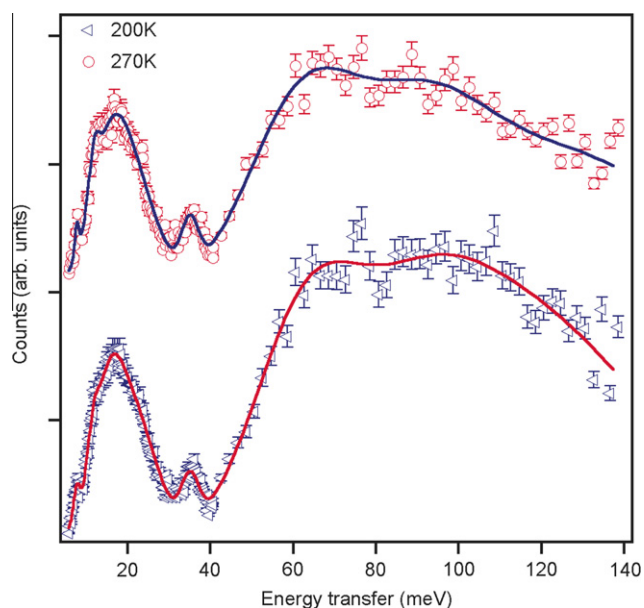


Fig. 2. Inelastic neutron scattering spectra for $\{\text{Mo}_{72}\text{Fe}_{30}\}$ nanocapsules at 270 K and 200 K. The continuous lines represent the overall fit using eight Gaussian components as analytically expressed by Eq. (2). The scatter of the data point is an indication of the experimental uncertainty.

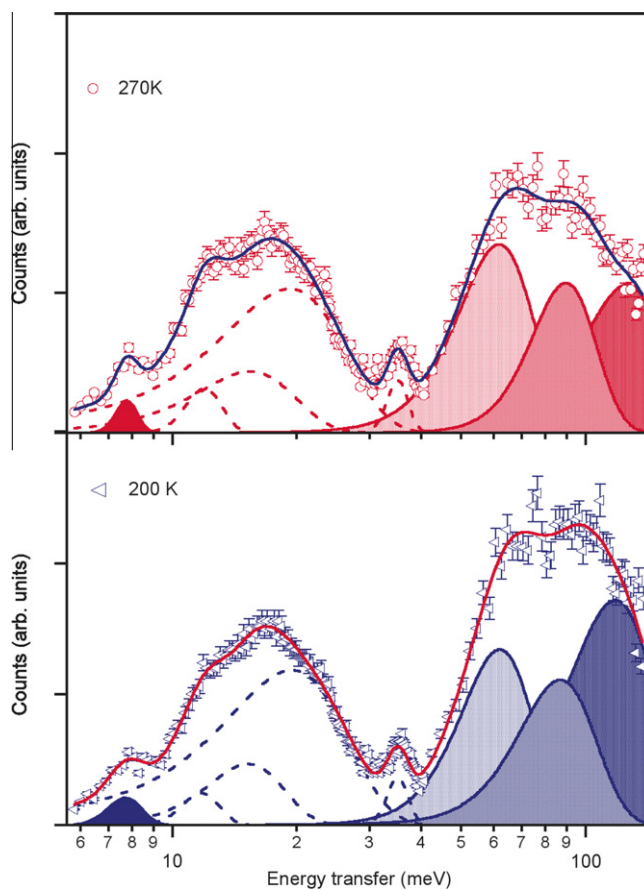


Fig. 3. Semi-log representation of $\{\text{Mo}_{72}\text{Fe}_{30}\}$ nanocapsules INS spectra registered at 270 K and 200 K showing the eight Gaussian components used in the fitting. The dotted lines refer to the four individual components ascribed to methyl groups present in the acetate ligand, while the solid filled components are connected to the water molecule modes and the continuous lines represent the overall fit. The scatter of the data point is an indication of the experimental uncertainty.

Fig. 3 shows the eight deconvoluted Gaussian bands at 270 K as well as their change when the sample temperature is decreased down to 200 K. The extracted parameters are listed in Table 1. The translational mode at 7.7 meV (see Table 1) is present in both spectra. This band is reminiscent of the two-peak structure already reported in supercooled water as obtained by molecular dynamic simulations [17]. As already anticipated the presence of the acetate ligand makes the extraction of the second translational band at

Table 1

Fitting parameters (amplitudes A_n , center frequency E_n , and σ_n) as extracted by the best fit using the eight components Gaussian deconvolution of the INS spectra of water contained in $\{\text{Mo}_{72}\text{Fe}_{30}\}$ nanocapsules at 270 K and 200 K. Parameters for components from 2 to 5 are not reported since they are not relevant for the present discussion.

	270 K	200 K
A_1	1.35	1.91
E_1 (meV)	7.8	7.7
σ_1 (meV)	0.47	0.72
A_6	205	209
E_6 (meV)	61	62
σ_6 (meV)	12.8	12.4
A_7	254	270
E_7 (meV)	89	87
σ_7 (meV)	17.1	18.4
A_8	350	600
E_8 (meV)	128	119
σ_8 (meV)	27.3	28.1

about 20 meV impractical. The region between 40 meV and 140 meV can be well fitted using three Gaussians related to the three rotational modes (librations), as already shown by Crupi et al. [18]. In this region the contribution of the methyl group is nearly negligible. In case of Gelsil matrix the librations are centered at about 52 meV, 70 meV and 91 meV while in the present case the librations are shifted to slightly higher frequencies (from 10 meV to 35 meV, see Table 1). This prominent shift is due to the higher confinement imposed by the interaction between the water molecules and the $\{\text{Mo}_{72}\text{Fe}_{30}\}$ core.

3.2. Self-assembly in aqueous solution

The self-assembly of $\{\text{Mo}_{72}\text{Fe}_{30}\}$ macroanions in vesicle-like “blackberry” structures in solution has been revealed and extensively monitored using static and dynamic laser light scattering techniques varying the initial concentration, pH, ionic strength and polarity of the solvent [2–6]. The blackberry formation of $\{\text{Mo}_{72}\text{Fe}_{30}\}$ in water is unusually slow: it takes months to reach thermodynamic equilibrium at room temperature, and can be accelerated increasing temperature [3–5]. It has been recently hypothesized that this aggregation process passes through a slow formation of oligomers and the presence of salts can increase the lag period of monomer to vesicle transition [6]. Due to the high X-ray contrast between the nanocapsule and water, SAXS is the perfect technique to study this transition and can even reveal the presence of oligomers in the presence of monomers/vesicles. Fig. 4 shows the SAXS intensity distribution for a 0.5 mg/mL $\{\text{Mo}_{72}\text{Fe}_{30}\}$ aqueous solution after: preparation (lower panel) and one month of aging at 25 °C (upper panel). As time passes the low- Q SAXS intensity increases as in the case of light scattering techniques giving evidence of the presence of large aggregates. It is important to stress that within the given Q range (from 0.09 nm^{-1} to 5.5 nm^{-1}) we are able to perceive scattering objects with a total dimension from about $(\pi/5.5)$ 0.5 nm to about $(\pi/0.09)$ 35 nm, hence we can distinguish both nanocapsule with a diameter of 2.5 nm [1] and blackberry-like aggregate with total dimension in the range from 20 nm to 40 nm. Adopting a model independently approach, the radius of gyration (R_g)³ can be experimentally extracted from the scattering curve of a pure form factor using the well-know Guinier plot [23], $\ln I(Q)$ vs. Q^2 . When the Guinier approximation $I(Q) = K \exp(-Q^2 R_g^2/3)$ holds ($R_g Q_{\text{max}} < 1.3$) the R_g can be directly calculated by the slope of the linear regions present in the Guinier representation. The Guinier plots of the scattering curves reported in Fig. 4 are shown in Fig. 5 in the region from 0 up to 0.008 \AA^{-2} . Both curves present two linear regions according to the facts that the monomers and aggregates coexists in solution even in freshly prepared samples. The R_g values are obtained by linear fit of corresponding regions as evidenced in the Fig. 5. The highest Q used in the fitting does not satisfy the empirical criterion for Guinier fit, $R_g Q < 1.3$ only in the cases of the 1 month old solution so that the extracted R_g value will be referred to as ‘apparent’. The first important point is the obvious evidence of two different linear regions in the Guinier plot of the freshly prepared $\{\text{Mo}_{72}\text{Fe}_{30}\}$ aqueous solution. The R_g associated with the two lines are respectively, 1.1 nm and 3.1 nm. It is worthwhile to remember that a sphere of radius, R , results in an $R_g^2 = 3R^2/5$. Considering that the $\{\text{Mo}_{72}\text{Fe}_{30}\}$ has a global diameter of 2.5 nm [1] its R_g would be about 1 nm which is in complete agreement with the extracted value of 1.1 nm. Hence, the greater R_g of 3.1 nm corresponds to the coexistence of an oligomer of the investigated macroanions. If we repeat the same treatment on the aged sample the apparent R_g

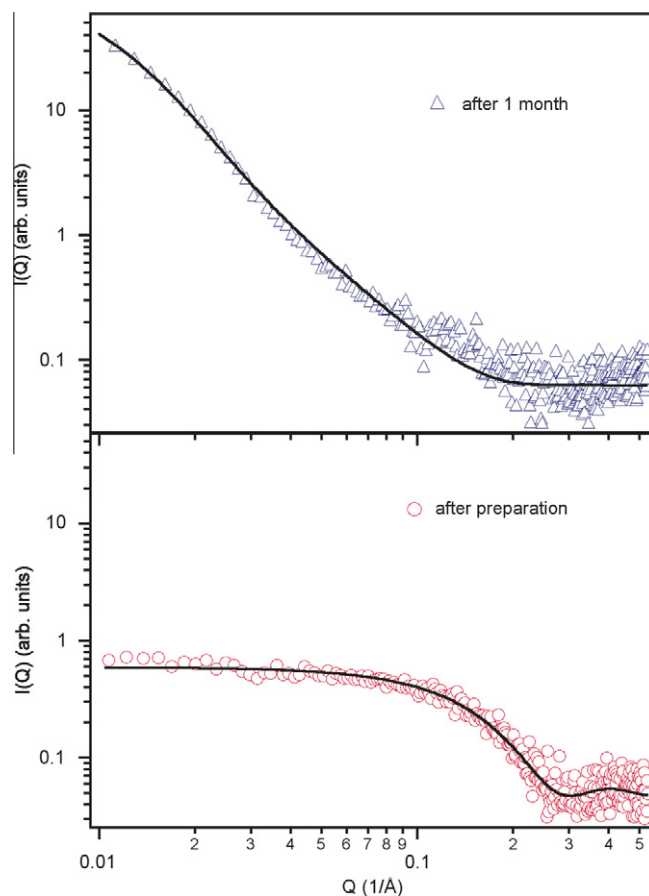


Fig. 4. Scattering curve of 0.5 mg/mL $\{\text{Mo}_{72}\text{Fe}_{30}\}$ nanocapsules water solution at 25 °C. Lower panel: (○) freshly prepared. Upper panel: (△) 1 month old. Continuous lines are the best fit according to the model described by Eq. (3).

as extracted by the Guinier plot is about 13 nm close to the theoretical value of about 18.8 nm calculated assuming a 40 nm blackberry-like hollow structure with a 2.5 nm wall thickness.⁴

In order to access the fine structure of the species present in solution and have a more exhaustive description, the scattering curves have been reconstructed using the following analytical approach. In both cases a spherical core–shell model has been implemented considering a polydispersity on the inner radius as described by a Schulz distribution, $G(r, Z)$:

$$I(Q) = \frac{1}{V} \int_0^\infty G(r_c, Z) F^2(Qr_c, t, \text{SLD}_i) dr_c + \text{bkg} \quad (3)$$

The fitting parameters are: inner radius of the capsule (r_c), polydispersity of inner radius ($p = 1/\sqrt{Z+1}$), thickness of the capsule (t), X-ray scattering length densities (SLD_i) [24] of the inner volume, of the capsule shell, and of the solvent and an instrumental background (bkg). Further details on Eq. (3) can be found in the literature [25]. This model is able to analytically describe a hollow structure when the SLD proper of the inner volume of the object is equal to the value proper of the solvent ($\text{SLD}_{\text{water}} = 9.4 \times 10^{-6} \text{ \AA}^{-2}$). Extracted fitting parameters for both samples are reported in table 2 and the fitting curves are represented by the solid lines shown in Fig. 4.

In the case of the fresh sample the scattering curve has been modeled considering only the monomer as the representative specie (polydispersity fixed to 0). In particular, the oligomer

³ In small angle X-ray scattering the radius of gyration is defined as the mean square distance from the center of gravity of the scattering object where the role of “mass” is played by the electrons.

⁴ The radius of gyration associated to a hollow sphere is: $R_g^2 = (3/5) \frac{(r_o^5 - r_i^5)}{(r_o^3 - r_i^3)}$.

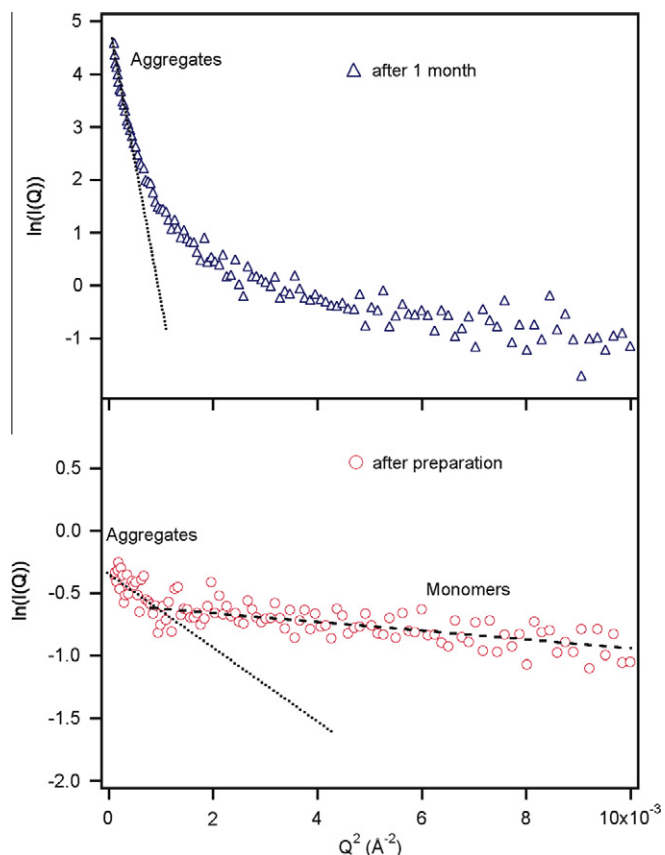


Fig. 5. Guinier plot of scattering curves reported in Fig. 4. Lower panel: (○) freshly prepared. Upper Panel: (Δ) 1 month old. Dashed line is the best fit according to the Guinier approximation for $\{Mo_{72}Fe_{30}\}$ monomers. Dotted lines are the best fit according to the Guinier approximation for aggregates.

Table 2

Fitting parameters used to best fit the SAXS curves of: fresh $\{Mo_{72}Fe_{30}\}$ aqueous solution using the core shell form factor and the 1 month old sample using a Schulz distribution of core shell spherical objects.

	Fresh	1 Month
Inner radius (nm)	0.4 ± 0.1	4.6 ± 0.1
Polydispersity (p)	0^a	0.8
Shell thickness (nm)	0.9 ± 0.1	2.6^b
Inner volume SLD (10^{-6} \AA^{-2})	9.4^a	19
Shell SLD (10^{-6} \AA^{-2})	61.5	61.5^b
Water SLD (10^{-6} \AA^{-2})	9.4^a	9.4^b
bkg	0.13	0.13

^a These parameters have been fixed during the fitting procedure.

^b These parameters have been fixed to the values as extracted by the fitting on the fresh sample.

contribution is responsible for the excess of scattering at Q lower than 0.03 \AA^{-1} confirming our starting assumption. $\{Mo_{72}Fe_{30}\}$ nanocapsule in solution is “seen” by X-ray as a hollow structure with an inner radius of 0.4 nm and a thickness of 0.9 nm. The total diameter of $2(0.4 \text{ nm} + 0.9 \text{ nm}) = 2.6 \text{ nm}$ is in excellent agreement with the reported dimension of 2.5 nm [1].

In order to fit the aged sample two requirements need to be satisfied: the polydispersity need to be different from 0 (this means that the aggregates have a broad distribution of dimensions) and the inner volume SLD must have a value greater than the value proper of the solvent in order to take into account that some monomer can be trapped inside the final blackberry-like aggregates. Final average size of the aggregates results in

$2 \times (4.6 \text{ nm} + 2.7 \text{ nm}) = 14.6 \text{ nm}$ which is much smaller than the value of 40 nm reported by Liu [3,4]. This is not surprising since this dimension has to be weighted with a Schulz distribution having $p = 0.8$ that results in a collection of object starting from few nanometers and vanishing for dimension bigger than about 60 nm.

4. Conclusions

Incoherent QENS and INS have been demonstrated as complimentary tools for the study of the water coordinated in voids between and inside the rather complex spherical $\{Mo_{72}Fe_{30}\}$ nanocapsule. This study has shown that the translational dynamics of the water molecules in the compound follows a non-Debye relaxation in contrast with that of bulk water at the same temperature. The temperature dependence of the relaxation time follows an Arrhenius law, indicating that the dynamics is triggered mainly by the breaking of the bonds connecting the crystal water molecules with the hydrophilic $\{Mo_{72}Fe_{30}\}$ surfaces. Inelastic neutron scattering spectra show an attenuation of water translational modes as compared to bulk water due to the strong destructuring effect imposed by the nanocage interface. Small angle X-ray scattering on freshly prepared aqueous solution (3 h) evidences the presence of the monomers (2.6 nm in diameter) that coexist with a small amount of oligomers (about 7 nm in diameter). After 1 month the polyoxomolibdate specie self-assembles in a supramolecular structure with a polydisperse distribution of dimensions spanning from the monomer (few nm) to the “blackberry” vesicular structure (up to 60 nm) already reported in Ref. [5].

Acknowledgments

The authors are grateful to Prof. A. Muller for stimulating comments on the subject. The authors wish also to thank Dr. T. Jenkins and Dr. J. Copley for assistance during the QENS measurements, Dr. Y. Liu and Dr. T. Udovic for assistance during the experiment on FANS and Dr. P. Luciani for assistance during the SAXS experiment. This work utilized facilities supported in part by the National Science Foundation under Agreement DMR-0454672. E.F. and P.B. also acknowledge financial support from the Consorzio Interuniversitario per lo Sviluppo dei Sistemi a Grande Interfase (CSGI) and the Ministero dell’Istruzione, Università e della Ricerca Scientifica (MIUR-prin 2008).

References

- [1] D.L. Long, E. Burkholder, L. Cronin, *Chem. Soc. Rev.* 36 (2007) 105.
- [2] T. Liu, B. Imber, E. Diemann, G. Liu, K. Cokleski, H. Li, Z. Chen, A. Müller, *J. Am. Chem. Soc.* 128 (2006) 15914.
- [3] T. Liu, *J. Am. Chem. Soc.* 124 (2002) 10942.
- [4] T. Liu, *J. Am. Chem. Soc.* 125 (2003) 312.
- [5] G. Liu, T. Liu, *J. Am. Chem. Soc.* 127 (2005) 6942.
- [6] J. Zhang, D. Li, G. Liu, K.J. Glover, T. Liu, *J. Am. Chem. Soc.* 131 (2009) 15152.
- [7] A. Müller, S. Sarkar, S.Q.N. Shah, H. Bögge, M. Schmidtman, S. Sarkar, P. Kögerler, B. Hauptfleisch, A.X. Trautwein, V. Schünemann, *Angew. Chem., Int. Ed. Engl.* 38 (1999) 3238.
- [8] J.R.D. Copley, J.C. Cook, *Chem. Phys.* 292 (2003) 477.
- [9] A. Meyer, R.M. Dimeo, P.M. Gehring, D.A. Neumann, *Rev. Sci. Instrum.* 74 (2003) 2759.
- [10] A. Faraone, E. Fratini, A.M. Todea, B. Krebs, A. Müller, P. Baglioni, *J. Phys. Chem. C* 113 (2009) 8635.
- [11] T.J. Udovic, D.A. Neumann, J. Leão, C.M. Brown, *Nucl. Instrum. Methods A* 517 (2004) 189.
- [12] J.R.D. Copley, D.A. Neumann, W.A. Kamitakahara, *Can. J. Phys.* 73 (1995) 763.
- [13] M. Lagi, P. Lo Nostro, E. Fratini, B.W. Ninham, P. Baglioni, *J. Phys. Chem. B* 111 (2007) 589.
- [14] T. Blanton, T.C. Huang, H. Toraya, C.R. Hubbard, S.B. Robie, D. Louer, H.E. Gobel, G. Will, R. Gilles, T. Raftery, *Powder Diffr.* 10 (1995) 91.
- [15] J.A. Lake, *Acta Crystallogr.* 23 (1967) 191.
- [16] H. Prask, H. Boutin, S. Yip, *J. Chem. Phys.* 48 (1968) 3367.

- [17] S.H. Chen, C. Liao, F. Sciortino, P. Gallo, P. Tartaglia, *Phys. Rev. E* 59 (1999) 6708.
- [18] V. Crupi, D. Majolino, P. Migliardo, V. Venuti, A.J. Dianoux, *Appl. Phys. A* 74 (2002) S555.
- [19] A. Faraone, E. Fratini, P. Baglioni, S.H. Chen, *J. Chem. Phys.* 121 (2004) 3212.
- [20] A. Rahman, F.H. Stillinger, *J. Chem. Phys.* 55 (1971) 3336.
- [21] <<http://www.wisis2.isis.rl.ac.uk/insdatabase/Results.asp?Acetone>>.
- [22] M.C. Bellisent-Funel, S.H. Chen, J.M. Zanotti, *Phys. Rev. E* 51 (1995) 4558.
- [23] G. Porod, in: O. Glatter, O. Kratky (Eds.), *Small Angle X-ray Scattering*, Academic Press, New York, 1982, p. 25.
- [24] <<http://www.ncnr.nist.gov/resources/sldcalc.html>>.
- [25] M. Bonini, E. Fratini, P. Baglioni, *Mater. Sci. Eng. C* 27 (2007) 1377 (and references therein).